

J.M. Molines  
Dpto. de Hidráulica-Escuela Civil  
Facultad de Ingeniería-Universidad del Zulia  
Maracaibo - Venezuela

Section Ondes et Marées  
Institut de Mécanique de Grenoble  
Francia

## SOME ASPECTS OF A TWO-LAYER, SHALLOW WATER NON-LINEAR INTERNAL WAVE, IN A RECTANGULAR TANK

### ABSTRACT

Equations of motion are developed in the general frame of the shallow water theory and for the case of a two-dimensional two-layer irrotational fluid. The solution is expressed as a cnoidal internal wave and solitary wave is found as a limit.

Laboratory experiments were carried out in a two-dimensional oscillating tank, to test the validity of the theoretical solution.

### RESUMEN

Las ecuaciones de movimiento se han desarrollado de acuerdo a la teoría de agua poco profunda en el caso de fluidos irrotacionales en dos capas. La solución se expresa como una onda cnoidal interna y en el límite se consigue una onda solitaria.

Se llevaron a efecto experimentos en laboratorio en un tanque bidimensional oscilatorio para verificar la validez de la solución teórica.

### I) INTRODUCTION

The study of internal waves has been carried out since many years by the "waves and Tides section" of the Institut de Mécanique of Grenoble. The previous works dealt with linear internal waves in a two-layer fluid, taking into account the effects of rotation. The results of Suberville (1974) have shown a very good agreement between the theory and the experiments. This linear theory was only relevant for the case where the depth of the upper and lower layer were equal ( $H_1=H_2$ ). In the other cases, ( $H_1 \neq H_2$ ), the phenomenon is very different, and the theoretical development must include non-linear terms. The case of a non-linear internal wave is now studied, omitting the effects of rotation. (The study with rotation will be performed later).

The equation of motion are developed in the general frame of the shallow water theory, according to the results of Germain (1967) and Helal (1979).

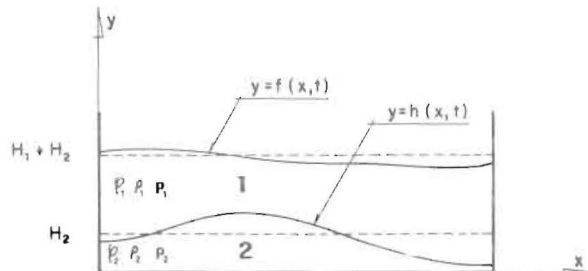
This expansion method leads to an analytic solution for the first order term, expressed with a Jacobi elliptic function sn.

Experiments were carried out to test the validity of the solution. Some observed peculiar features are then detailed.

### II) APPLICATION OF THE SHALLOW WATER THEORY TO THE CASE OF A TWO-LAYER FLUID.

#### 1) Notation :

The notations are precised on Fig.1.



— Fig. N° 1 —

#### 2) Equation of motion :

Using the Euler representation, the general equations can be written for each layer, using the irrotational assumption :

##### a) Dynamic equation :

$$\nabla^2 \left[ \frac{\partial \phi_i}{\partial t} + \frac{1}{2} \left[ \left( \frac{\partial \phi_i}{\partial x} \right)^2 + \left( \frac{\partial \phi_i}{\partial y} \right)^2 \right] + gy + \frac{P_i}{\rho_i} \right] = 0 \quad (i=1,2) \quad (1)$$

b) Kinematic equation :

$$\frac{\partial^2 \phi_i}{\partial x^2} + \frac{\partial^2 \phi_i}{\partial y^2} = 0 \quad (i=1,2) \quad (2)$$

c) Boundary conditions :

The boundary conditions are of two types.

i) At rigid boundaries, the normal velocity vanishes and we have :

- at the bottom

$$\frac{\partial \phi_2}{\partial y} = 0 \quad y=0 \quad (3)$$

- at the ends of the tank

$$\frac{\partial \phi_i}{\partial x} = 0 \quad \left[ \begin{array}{l} x=0 \\ x=L \end{array} \right] \quad (i=1,2) \quad (4)$$

ii) At free boundaries (free surface and interface) two conditions are imposed :

- a pressure condition which expressed that the free surface is an isobaric surface and that the pressure is the same on both sides of the interface (no superficial tension).  
According to (1) these conditions lead to the following equations :

$$\left\{ \frac{\partial \phi_1}{\partial t} + \frac{1}{2} \left[ \left( \frac{\partial \phi_1}{\partial x} \right)^2 + \left( \frac{\partial \phi_1}{\partial y} \right)^2 \right] \right\}_{y=f(x,t)} + g f(x,t) = Cte \quad (5)$$

$$1 \left\{ \frac{\partial \phi_1}{\partial t} + \frac{1}{2} \left[ \left( \frac{\partial \phi_1}{\partial x} \right)^2 + \left( \frac{\partial \phi_1}{\partial y} \right)^2 \right] + g h(x,t) + C_1 \right\}_{y=h(x,t)} =$$

$$2 \left\{ \frac{\partial \phi_2}{\partial t} + \frac{1}{2} \left[ \left( \frac{\partial \phi_2}{\partial x} \right)^2 + \left( \frac{\partial \phi_2}{\partial y} \right)^2 \right] + g h + C_2 \right\}_{y=h_1(x,t)} \quad (6)$$

- a velocity condition which expressed that the free surface and the interface are impervious :

$$\frac{\partial \phi_1}{\partial y} = \frac{\partial f}{\partial x} \frac{\partial \phi_1}{\partial x} + \frac{\partial f}{\partial t} \quad y = f(x,t) \quad (7)$$

$$\frac{\partial \phi_i}{\partial y} = \frac{\partial h}{\partial x} \frac{\partial \phi_i}{\partial x} + \frac{\partial h}{\partial t} \quad y = h(x,t) \quad (8)$$

(i = 1,2)

3) Parameters distortion and solution.

We now introduce the new variables

$$\bar{x} = \epsilon x$$

$$\bar{y} = y$$

$$\tau = \epsilon t$$

where  $\epsilon$  is a small stretching parameter. As  $\epsilon$  is small, the different unknown can be expanded in asymptotic expansion :

$$\phi_i = \sum_0^{\infty} \epsilon^{2n+1} \phi_i^{(2n+1)} \quad (10)$$

$$f(\bar{x}, \tau) = \sum_0^{\infty} \epsilon^{2n} f^{(2n)}(\bar{x}, \tau) \quad (11)$$

$$h(\bar{x}, \tau) = \sum_0^{\infty} \epsilon^{2n} h^{(2n)}(\bar{x}, \tau) \quad (12)$$

Then, using the standard procedure of this method, as shown with many details in (Helal & Molines, (1981)), we arrive at the final result :

$$h^{(2)}(\bar{x}, \tau) = \frac{(\rho_1 - \lambda \rho_2)}{g(P_2 - P_1)} \operatorname{ca} \left\{ \left( \frac{3k^2}{1+k^2} \right) [\operatorname{sn}^2(N(\bar{x} - c\tau), k^2) + \operatorname{sn}^2(N(\bar{x} + c\tau), k^2)] - 2 \right\} \quad (13)$$

where

$$N = \frac{1}{2} \sqrt{\frac{-3A\alpha}{1+k^2}}$$

All the parameters introduced in this relation are calculable since the physical parameters of the interface are known, namely  $H_1, H_2, \rho_1, \rho_2$ . (cf. Helal & Molines (1981)). More precisions are given in appendix I.  
This first order solution will now be compared with laboratory experiments.

### III) EXPERIMENTAL INSTALLATION

We have used the installation previously utilized by Suberville and described in (Chabert d'Hieres & Suberville (1974)). A synoptic diagram of the installation is shown in Fig. 2. Mainly there are three distinctive parts :

1) a mechanical part.

This part is mainly constituted by an oscillating tank (or canal) and its system of motion. The tank oscillates around an horizontal axis with an amplitude and a period which can be regulated by the system of motion.

2) a hydraulic part.

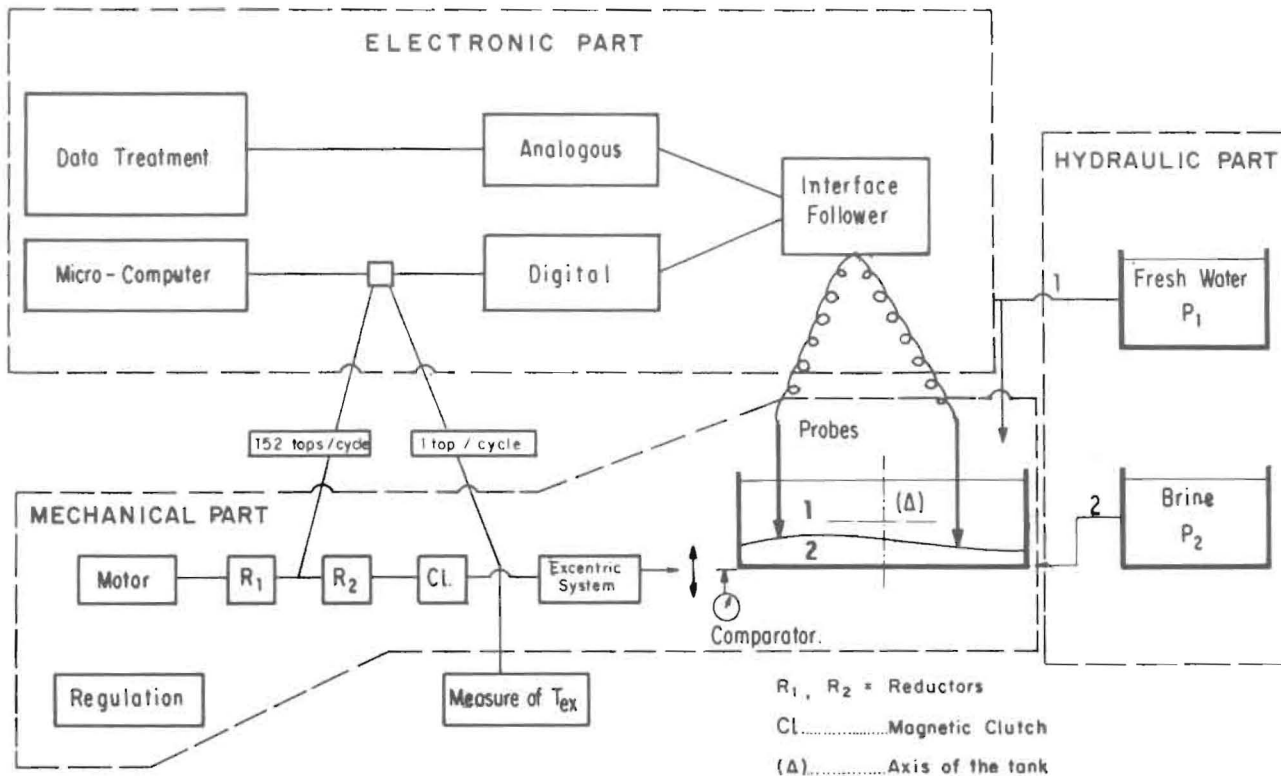
Two tanks containing fresh, ungasated water and brine respectively allow the filling of the canal

with two layers of fluid.

The brine, whose density is adjusted in the outside tank, is injected through the bottom of the canal. With this system of injection, the interface thickness is almost constant and about 6 mm.

3) an electronic and informatic part.

Informations from the internal wave are gathered using an interface follower. This apparatus, which is roughly an enslaved conductivitymeter, is able to follow a layer of given conductivity with a great accuracy :  $\pm 0.1$  mm for the interface level at about 1/3 s. Recording can be done both directly by a micro-computer and on a graphic recorder. A signal is generated in synchronism with the tank movement. Data are taken by the computer at a sample of 152 points per period.



— Fig. N° 2 —

#### IV) EXPERIMENTAL RESULTS

We will present here, the most typical experimental results that we found. The first one deals with the effect of the tank oscillation on the standing wave. The second one shows that a very good agreement between theory and experiments is found in a large range of the characteristic parameters. Finally, the third one precises the experimental suitable conditions to generate multi-soliton internal wave in our tank.

##### 1) Effect of the tank oscillation on the wave.

The internal wave is generated in the tank when this one is rocked around its axis at a period  $T_{ex}$ , which is as near as possible of the eigen baroclinic period of the tank,  $T_p$ . Obviously, as we deal with non-linear waves,  $T_p$  greatly depends on the wave amplitude  $A_i$  of the internal wave.

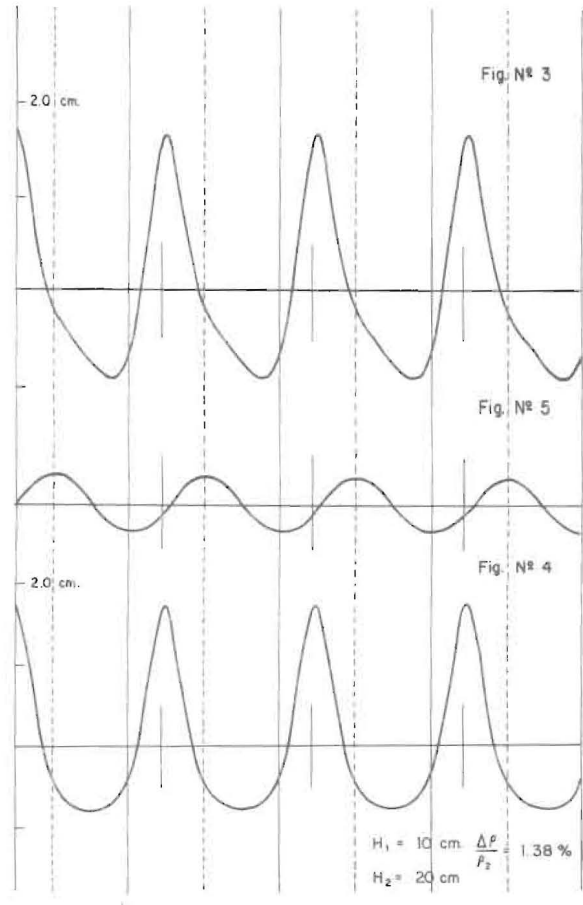
In order to determine if, whether or not,  $T_{ex} = T_p$ , we introduce the notion of phase-shift between the wave and the oscillation. The condition  $T_{ex} = T_p$  is realized when the wave and the oscillation of the tank are in quadrature, i.e. when the phase-shift is  $90^\circ$ . We will see in 3) what are the effects on the wave shape when this condition is not realized.

We must note here, that this way of determining  $T_{ex}$  is very accurate because the phase-shift is a very sensitive parameter. Practically, for a given amplitude of the wave, we modify the  $T_{ex}$  until the condition on the phase-shift is filled. In the following and in 2)  $T_{ex}$  is supposed to follow these conditions.

We have experimentally shown that the measured wave (Fig. 3) can be interpreted as a superposition of a main cnoidal wave (Fig. 4) with a small amplitude sine shape wave (Fig. 5). This last wave is supposed to be linked with the tank movement because it has a  $0^\circ$  phase-shift with the tank movement. On the other hand, the main cnoidal wave (Fig. 4) has a  $90^\circ$  phase-shift with the tank movement. But a more interesting feature is that the sine shape wave can be estimated by measuring the wave when the excitation period  $T_{ex}$  is about 10% less than the eigen period  $T_p$ . So if we measure the wave  $W_1$  when  $T_{ex} = T_p$  and then the wave  $W_2$  when  $T_{ex} = 90\% T_p$  we can compute the wave  $W = W_1 - W_2$ . We will serve as a basis for the comparison with the theoretical solution. The difference  $W_1 - W_2$  is computed points by points for each value.

##### 2) Comparison between $W$ and the theoretical solution.

From (13) it can be seen that the wave-length of the theoretical solution is



$$\Lambda = 4K(k) \sqrt{\frac{-(1+k^2)}{3A\alpha}} \quad (14)$$

The theoretical wave amplitude at one end of the tank is given by the relation

$$A_T = \frac{6k^2}{(1+k^2)} \frac{c\alpha(\rho_1 - \lambda\rho_2)}{g(\rho_2 - \rho_1)} \quad (15)$$

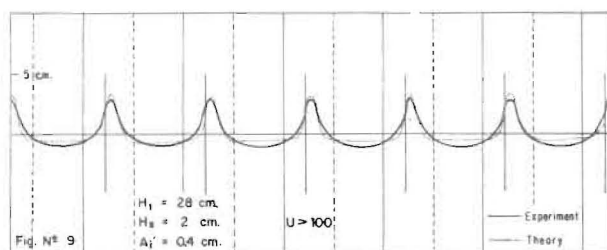
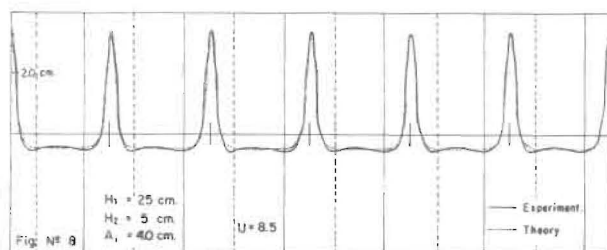
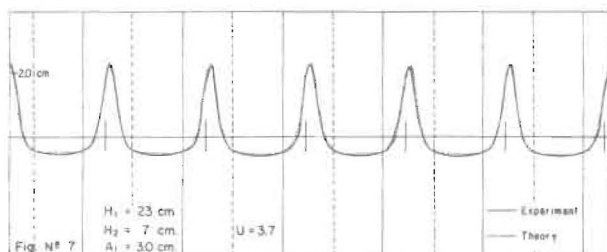
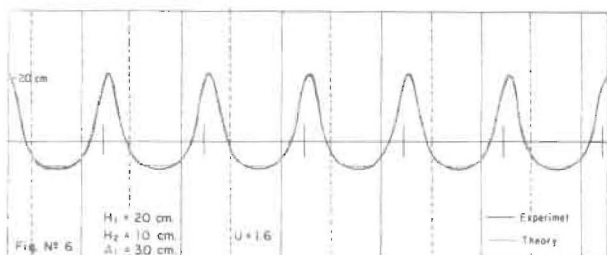
As we have a standing wave  $\Lambda = 2L$  where  $L$  is the length of the tank. The physical wave amplitude is known from the experiments and we impose  $A_i = A_T$ . So finally, we have the relation :

$$K^2 k^2 = \frac{A_i^2 \Lambda^2 A g (\rho_2 - \rho_1)}{32 c (\lambda \rho_2 - \rho_1)} \quad (16)$$

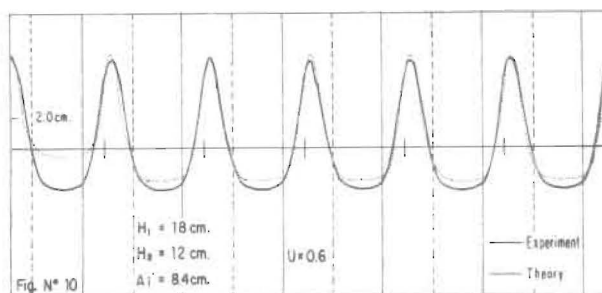
Since the function  $K^2 k^2(k^2)$  is bijective, relation (16) leads to a well defined value of  $k^2$  and then we are able to compute  $h_2$  from (13). Some comparison are shown in fig. 6 to fig. 10.

For certain experiments the agreements is quite perfect (Fig. 6 - 7 - 8). On the other hand, in some extreme experimental conditions, the comparison is not so good. The interpretation of

these differences differs if we are in a strongly non-linear area or at the opposit, in a slightly non-linear or quasi linear case. It has been shown by many Authors (e.g. Lee & Beardsley (1974)) that the solitary wave evolves from a balance between non-linear effects and dispersive effects. The ratio of the non-linear effects to the dispersive effects (Ursell number  $U$ ) give us an evaluation of this balance. For very high Ursell number (Fig. 9), the non-linear terms of higher order are not negligible and this explains the shape of the difference. (A calculus, made by Laitone (1960) of the higher terms for a surface wave had shown such a behaviour.)



At the opposit, for small Ursell number, (Fig. 10), the influence of dispersion is to spread out the wave and the calculations give us a thinner wave. This latter effect is not so clear and additional experiments are to be done to conclude further on.



### 3) Multi-soliton internal wave.

It is well known now (e.g. Hammack & Segur (1974), that solitary waves tends to break in packet of solitons under certain conditions. This is true for surface wave but also for internal wave as many observations in the nature have shown (e.g. Apel & Al. (1973), Osborne & Burch (1980)). In the case of a progressive wave, since the works of Gardner & Al. (1967), it is possible to calculate the fission of a solitary wave using the inverse scattering method.

In our case, where we have a standing wave, in an oscillating tank, the boundary conditions raise some mathematical difficulties because all the boundaries are moving. So, the mathematical work is no longer developed and, here, we are only giving experimental results.

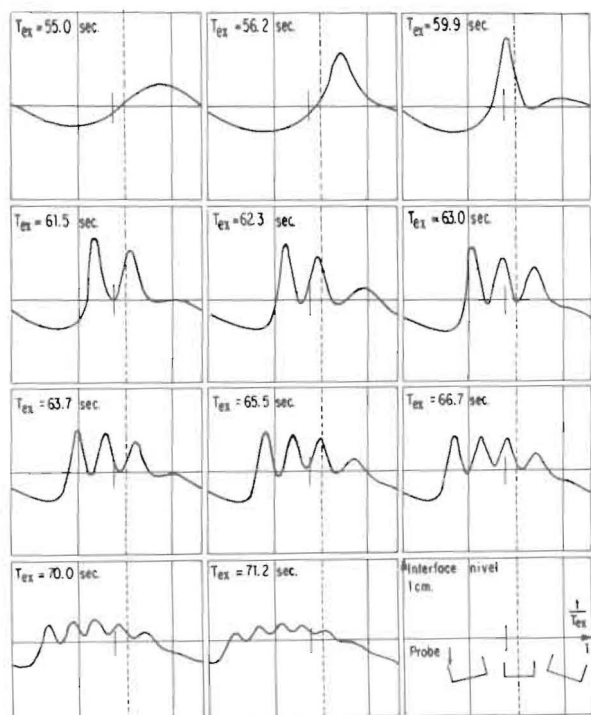
In fig. 11, we present different recording of the internal wave in function of time. The only parameter which changes from one draw to another is the exitation period. The following features are brought to attention :

- For  $T_{ex} = T_p$ , only one solitary wave envelopes and it can be described by the theory (cf §2).
- If  $T_{ex}$  increase, there is a fission of the solitary wave into numerous internal solitons and the phenomenon get stronger and atronger for increasing  $T_{ex}$ . On the order hand the wave amplitude decreases a little.
- Now, if  $T_{ex}$  decreases (in comparison with  $T_p$ ), the opposit phenomenon occurs : the wave amplitude decreases and the internal wave slightly takes the shape of a sine wave, as mentioned above (for  $T_{ex} = 90\% T_p$ ).

Also of note is the phase-shift of the wave. In the right lower corner of fig. 11, we give a diagram of the position of the tank during a period of oscillation, and the vertical lines are related with the extreme positions of the tank movement.

When  $T_{ex}$  increases, the phase shift increases. When  $T_{ex}$  decreases, the phase shift decreases and is nearly 0 for  $T_{ex}=90\% T_p$ .

These results demonstrate the great importance of  $T_{ex}$  for experiments as described in § 2.



- Fig. N° 11 -

$H_1 = 24$  cm.  
 $H_2 = 6$  cm.  $T_p = 58.1$  sec.  
 $\frac{\Delta \rho}{\rho} = 1.34\%$

#### V) CONCLUDING REMARKS

We have seen that the theoretical works of Germain (1967) and Helal (1979) have found a good confirmation for numerous experiments.

To complete this work, it will be interesting to solve the problem of the moving boundaries and to extend this study to the rotating fluids. The study of this latter problem will be performed in a larger tank. A similitude with Ocean motion will be possible then, including the effects of Earth's rotation on the flow.

#### REFERENCES

- 1) ABRAMOWITZ M. : "Hand Book of Mathematical Functions". (1956).
- 2) APEL J.R., BYRNE H.M., PRONI J.R., CHARNELL R.L. "Observations of oceanic internal and surface waves from Earth Resources Technology Satellite". (1973). J. Geophys. Res. 80(6): 865-881.

- 3) CHABERT D'HIERES G., SUBERVILLE J.L. : "Ondes Internes dans un bassin rectangulaire tournant". (1974). La Houille Blanche 7/8 : 623-630.
- 4) GARDNER C.S., GREENE J.M., KRUSKAL M.D., MIURA R.M. : "Method for solving the Korteweg - De Vries equation". (1967). Phys. Rev. Lett. 19 : 1095-1097.
- 5) GERMAIN J.P. : "Contribution à l'étude de la houle en eau peu profonde". (1967). Thèse faculté des Sciences de Grenoble.
- 6) HAMMACK J.L., SEGUR H. : "The Korteweg-De Vries equation and Water Waves. Part 2 : Comparison with experiments". J. Fluid. Mech. 65 : 289-314 (1974).
- 7) HELAL M.A. : "Application de la théorie de l'eau peu profonde au cas des fluides en bicouches et aux fluides tournants". (1979). Thèse Université de Grenoble.
- 8) HELAL M.A., MOLINES J.M. : "Non-linear internal waves in shallow water : A theoretical and experimental study". (1981). Tellus 33(3) : 488-504.
- 9) LAITONE E.V. : "Second order cnoidal surface waves". (1960). J. Fluid. Mech. 9:430-444.
- 10) LEE C.Y., BEARDSLEY R.C. : "The generation of long non-linear internal waves in a weakly stratified shear flow". (1974). J. Geophys. Res. 79(3) : 459-462.
- 11) OSBORNE A.R., BURCH T.L. : "Internal solitons in the Andaman sea". (1980). Sciences 208-4443: 451-460.
- 12) SUBERVILLE J.L. : "Ondes internes en fluides tournants, Contribution théorique et expérimentale". (1974) Thèse Université de Grenoble.

#### VI APPENDIX

Eq. 13 gives us the expression of  $h^2$ :

$$h^2(\bar{x}, \tau) = \left[ \frac{\rho_1 - \lambda \rho_2}{g(\rho_1 - \rho_2)} \right] \text{ca} \left( \frac{3k^2}{1+k^2} \right) \left[ \text{sn} (N(\bar{x}-c\tau), k^2) + \text{sn}^2 (N(\bar{x}+c\tau), k^2) \right] - 2 \quad (13)$$

In this equation, we deal with the elliptic Jacobi function  $\text{sn}$ , which depends on two parameters :  $\text{sn} (u, k^2)$ . The first one is a time-type parameter. The second one is a shape parameter. For  $k^2=0, \text{sn}(u,0)=\sin(u)$ , (sine shape wave) and for  $k^2 = 1, \text{sn}(u,1)=1+\text{th}^2(u)$  (solitary-wave shape).

For a particular case, parameter  $k^2$  is implic-

itly determined from the wave length  $\lambda$  and from the internal wave amplitude  $A_{in}$ .

In fact we have :

$$(A-1) \quad A_{in} = 6 \left( \frac{\rho_1 \lambda \rho_2}{g(\rho_1 - \rho_2)} \right) \alpha c \frac{k^2}{1+k^2}$$

$$(A-2) \quad \lambda = 4K \sqrt{\frac{(1+k^2)}{-3A\alpha}}$$

where  $K$  is the complete elliptic integral of the first kind.

Parameters  $A, \lambda, c$  depend only of physical parameters, as follow :

$$(A-3) \quad H_0 = H_1 + H_2$$

$$(A-4) \quad c^2 = \frac{1}{2} g \left[ H_0 - \sqrt{H_0^2 - 4H_1 H_2 \frac{\Delta\rho}{\rho_2}} \right]$$

$$(A-5) \quad \gamma = H_0 + \frac{c^2}{g}$$

$$(A-6) \quad \lambda = \frac{c^2 - gH_1}{gH_2}$$

$$(A-7) \quad A = - \frac{M_2}{3M_1} \quad \text{where}$$

$$(A-8) \quad M_1 = \left[ \frac{c^2 \rho_2}{g(\rho_2 - \rho_1)} \right] \left[ \frac{\lambda H_2^3}{6} - \frac{c^2 H_2}{2g(\rho_2 - \rho_1)} \{ \lambda H_2 \rho_2 + \rho_1 (2\gamma - H_2) \} - \left( H_2 - \frac{c^2 \rho_2}{g(\rho_2 - \rho_1)} \right) \left[ \frac{H_0^3 - H_2^3}{6} - \frac{\gamma}{2} (H_0^2 - H_2^2) - \frac{c^2}{2g} \left( H_0 + \frac{H_2^2 (\rho_1 - \lambda \rho_2)}{(\rho_2 - \rho_1)} \right) + \frac{c^2 \rho_2}{g} \left( H_0 + \frac{H_2 \rho_1}{\rho_2 - \rho_1} \right) \right] \right]$$

$$(A-9) \quad M_2 = \frac{c^3 \rho_2}{[g(\rho_2 - \rho_1)]^2} \left[ -3\lambda^2 \rho_2 + 2\lambda \rho_1 + \rho_1 \right] - \left( H_2 - \frac{c^2 \rho_2}{g(\rho_2 - \rho_1)} \right) \left( \frac{c \rho_2 (\lambda + 3) (\lambda - 1)}{g(\rho_2 - \rho_1)} \right)$$

Elimination of  $\alpha$  between eq. (A-1) and (A-2) gives the following equation :

$$(A-10) \quad K^2 k^2 = \frac{\lambda^2 A A_{in} g (\rho_2 - \rho_1)}{16 c (\rho_1 - \lambda \rho_2)}$$

The function  $K^2 k^2$  is bijective function so that eq. (A-10) defines implicitly only value of  $k^2$ . Then, using this value in eq.(A-1) we get  $\alpha$ .

Computation of elliptic functions can be done following algorithm given in ABRAMOVITZ's hand-book of mathematical functions.

Recibido el 1º de febrero de 1984